

# Exclusive photoproduction of $\Upsilon$ : from HERA to Tevatron

A. Rybarska,<sup>1,\*</sup> W. Schäfer,<sup>1,†</sup> and A. Szczurek<sup>1,2,‡</sup>

<sup>1</sup>*Institute of Nuclear Physics PAN, PL-31-342 Cracow, Poland*

<sup>2</sup>*University of Rzeszów, PL-35-959 Rzeszów, Poland*

(Dated: July 22, 2008)

## Abstract

The forward photoproduction amplitude for  $\gamma p \rightarrow \Upsilon p$  is calculated in a pQCD  $k_{\perp}$ -factorization approach with an unintegrated gluon distribution constrained by inclusive deep-inelastic structure functions. The total cross section for diffractive  $\Upsilon$ s is compared with a recent HERA data. We also discuss the  $2S/1S$  ratio in diffractive  $\Upsilon$ -production. The amplitude is used to predict the cross section for exclusive  $\Upsilon$  production in hadronic reactions. Differential distributions for the exclusive  $p\bar{p} \rightarrow p\Upsilon\bar{p}$  process are calculated for Tevatron energies. We also show predictions for LHC. Absorption effects are included.

PACS numbers: 13.60.Le, 13.85.-t, 12.40.Nn

---

\*Electronic address: Anna.Cisek@ifj.edu.pl

†Electronic address: Wolfgang.Schafer@ifj.edu.pl

‡Electronic address: Antoni.Szczurek@ifj.edu.pl

## I. INTRODUCTION

The inclusive production of quarkonia was studied intensively in the past both in elementary hadronic and nuclear reactions at SPS, RHIC and Tevatron energies. For a review see e.g.[1]. In contrast, the exclusive production of heavy  $Q\bar{Q}$  vector quarkonium states (e.g.  $h_1 h_2 \rightarrow h_1 \Upsilon h_2$ ) in hadronic interactions was never measured, but attracted recently much attention from the theoretical side [2, 3, 4, 5, 6, 7, 8]. Due to the negative charge-parity of the vector meson, the purely hadronic Pomeron–Pomeron fusion mechanism of exclusive meson production is not available, and instead the production will proceed via photon–Pomeron fusion. A possible purely hadronic mechanism would involve the elusive Odderon exchange [2, 6]. Currently there is no compelling evidence for the Odderon, and here we restrict ourselves to the photon–exchange mechanism, which exists without doubt, and must furthermore dominate any hadronic exchange at very small momentum transfers. In our approach to the exclusive hadronic reaction, we follow closely the procedure outlined in our previous work on  $J/\psi$  production [7]. There is one crucial difference, though. While in the case of diffractive  $J/\psi$  photoproduction there exist a large body of fairly detailed data, including e.g. transverse momentum distributions, the photoproduction data for exclusive  $\Upsilon$ ’s are rather sparse [9, 10, 11]. Hence, different from [7] we cannot avoid modelling the relevant  $\gamma p \rightarrow \Upsilon p$  subprocess. Fortunately, due to the large mass of the  $\Upsilon$ ’s constituents, the cross section gets its main contribution from small-size  $b\bar{b}$ -dipoles, and the production mechanism can be described in a pQCD framework (for a recent review and references, see [12]). The two main ingredients are the unintegrated gluon distribution of the proton, and the light–cone wave function of the vector meson. The unintegrated gluon distribution is sufficiently well constrained by the precise small- $x$  data for the inclusive proton structure function, and we shall content ourselves here with a particular parametrisation which provides a good description of inclusive deep inelastic scattering data [13]. As the relevant energy range of the  $\gamma p \rightarrow \Upsilon p$  subprocess at Tevatron overlaps well with the HERA energy range, any glue which fulfills the stringent constraints of the precise HERA  $F_2$ -data must do a similar job. Alternative unintegrated gluon distributions are discussed for example in [14].

The current experimental analyses at the Tevatron [15] call for an evaluation of differential distributions including the effects of absorptive corrections.

The HERA data cover the  $\gamma p$  center of mass (cm-) energy range  $W \sim 100 \div 200$  GeV. This energy range is in fact very much relevant to the exclusive production at Tevatron energies for not too large rapidities of the meson, say  $|y| \lesssim 3$ . This will be different at the LHC, where a broad range of subsystem energies  $W_{\gamma p}$ , up to several TeV, is spanned for  $\Upsilon$  emitted in the forward directions. This will require a long-range extrapolation to a completely new unexplored region. In this paper, however, we will concentrate on predictions for Tevatron energies. Here our input amplitude is constrained by the HERA data, to which description we now turn.

## II. PHOTOPRODUCTION $\gamma p \rightarrow \Upsilon p$ AT HERA

We thus turn to the analysis of the photoproduction reaction studied at HERA. The photoproduction amplitude will then be the major building block for our prediction of exclusive  $\Upsilon$  production at the Tevatron.

### A. Amplitude for $\gamma p \rightarrow \Upsilon p$

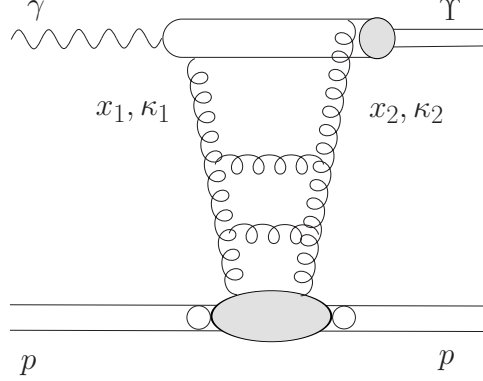


FIG. 1: A sketch of the exclusive  $\gamma p \rightarrow \Upsilon p$  amplitude.

The amplitude for the reaction under consideration is shown schematically in Fig.1. As it is explained in Ref.[12], the imaginary part of the amplitude for the  $\gamma^* p \rightarrow \Upsilon p$  process can be written as

$$\begin{aligned} \Im \mathcal{M}_{\lambda_\gamma, \lambda_V}(W, t = -\Delta^2, Q^2) &= W^2 \frac{c_\Upsilon \sqrt{4\pi\alpha_{em}}}{4\pi^2} \int \frac{d^2\kappa}{\kappa^4} \alpha_S(q^2) \mathcal{F}(x_1, x_2, \kappa_1, \kappa_2) \\ &\times \int \frac{dz d^2\mathbf{k}}{z(1-z)} I_{\lambda_\gamma, \lambda_V}(z, \mathbf{k}, \kappa_1, \kappa_2, Q^2), \end{aligned} \quad (2.1)$$

where the transverse momenta of gluons coupled to the  $Q\bar{Q}$  pair can be written as

$$\kappa_1 = \kappa + \frac{\Delta}{2}, \quad \kappa_2 = -\kappa + \frac{\Delta}{2}. \quad (2.2)$$

The quantity  $\mathcal{F}(x_1, x_2, \kappa_1, \kappa_2)$  is the off diagonal unintegrated gluon distribution. Explicit expressions for  $I_{\lambda_\gamma, \lambda_V}$  can be found in [12]. For heavy vector mesons, helicity-flip transitions may be neglected, and we concentrate on the  $s$ -channel helicity conserving amplitude,  $\lambda_\gamma = \lambda_V$ . In the forward scattering limit, i.e. for  $\Delta = 0$ , azimuthal integrations can be performed analytically, and we obtain the following representation for the imaginary part of the amplitude for forward photoproduction  $\gamma p \rightarrow \Upsilon p$ :

$$\Im \mathcal{M}(W, \Delta^2 = 0, Q^2 = 0) = W^2 \frac{c_\Upsilon \sqrt{4\pi\alpha_{em}}}{4\pi^2} 2 \int_0^1 \frac{dz}{z(1-z)} \int_0^\infty \pi dk^2 \psi_V(z, k^2) \quad (2.3)$$

$$\int_0^\infty \frac{\pi dk^2}{\kappa^4} \alpha_S(q^2) \mathcal{F}(x_{eff}, \kappa^2) \left( A_0(z, k^2) W_0(k^2, \kappa^2) + A_1(z, k^2) W_1(k^2, \kappa^2) \right), \quad (2.4)$$

where

$$A_0(z, k^2) = m_b^2 + \frac{k^2 m_b}{M + 2m_b}, \quad (2.5)$$

$$A_1(z, k^2) = \left[ z^2 + (1-z)^2 - (2z-1)^2 \frac{m_b}{M + 2m_b} \right] \frac{k^2}{k^2 + m_b^2}, \quad (2.6)$$

and

$$\begin{aligned} W_0(k^2, \kappa^2) &= \frac{1}{k^2 + m_b^2} - \frac{1}{\sqrt{(k^2 - m_b^2 - \kappa^2)^2 + 4m_b^2 k^2}}, \\ W_1(k^2, \kappa^2) &= 1 - \frac{k^2 + m_b^2}{2k^2} \left( 1 + \frac{k^2 - m_b^2 - \kappa^2}{\sqrt{(k^2 - m_b^2 - \kappa^2)^2 + 4m_b^2 k^2}} \right). \end{aligned} \quad (2.7)$$

To obtain these results, the perturbative  $\gamma \rightarrow b\bar{b}$  light cone wave function was used; the vertex for the  $b\bar{b} \rightarrow \Upsilon$  transition is given below, and is obtained by projecting onto the pure  $s$ -wave  $b\bar{b}$ -state. Here  $c_\Upsilon = e_b = -1/3$ , and the mass of the bottom quark is taken as  $m_b = 4.75$  GeV. The relative transverse momentum squared of (anti-)quarks in the bound state is denoted by  $k^2$ , their longitudinal momentum fractions are  $z, 1-z$ , and we introduced

$$M^2 = \frac{k^2 + m_b^2}{z(1-z)}. \quad (2.8)$$

The dominant contribution to the amplitude comes from the piece  $\propto A_0 W_0 \sim m_b^2 W_0$ , and our exact projection onto  $s$ -wave states differs in fact only marginally from the naive  $\gamma_\mu$ -vertex for the  $\Upsilon \rightarrow b\bar{b}$  transition. The 'radial' light-cone wave function of the vector meson,  $\psi_V(z, k^2)$  will be discussed further below. The unintegrated gluon distribution  $\mathcal{F}(x, \kappa^2)$  is normalized such that for a large scale  $\bar{Q}^2$  it will be related to the integrated gluon distribution  $g(x, \bar{Q}^2)$  through

$$xg(x, \bar{Q}^2) = \int^{\bar{Q}^2} \frac{d\kappa^2}{\kappa^2} \mathcal{F}(x, \kappa^2). \quad (2.9)$$

The running coupling  $\alpha_S$  enters at the largest relevant virtuality  $q^2 = \max\{\kappa^2, k^2 + m_b^2\}$ . Due to the finite mass of the final state vector meson, the longitudinal momentum transfer is nonvanishing, and, as indicated above, a more precise treatment would require the use of skewed/off-diagonal gluon distributions. At the high energies relevant here it is admissible to account for skewedness by an appropriate rescaling of the diagonal gluon distribution [17]. With the specific gluon distribution used by us, the prescription of [17] can be emulated by taking the ordinary gluon distribution at [12]

$$x_{eff} = C_{skewed} \frac{M_V^2}{W^2} \sim 0.41 \cdot \frac{M_V^2}{W^2}. \quad (2.10)$$

The full amplitude, at finite momentum transfer, well within the diffraction cone, is finally written as

$$\mathcal{M}(W, \Delta^2) = (i + \rho) \Im m \mathcal{M}(W, \Delta^2 = 0) \exp(-B(W) \Delta^2). \quad (2.11)$$

Here  $\Delta^2$  is the (transverse) momentum transfer squared,  $B(W)$  is the energy-dependent slope parameter:

$$B(W) = B_0 + 2\alpha'_{eff} \log \left( \frac{W^2}{W_0^2} \right), \quad (2.12)$$

with  $\alpha'_{eff} = 0.164 \text{ GeV}^{-2}$  [16],  $W_0 = 95 \text{ GeV}$ . For the value of  $B_0$  see the discussion of the numerical results below. For the small size  $b\bar{b}$  dipoles relevant to our problem, a fast rise of

the cross section can be anticipated, and it is important to include the real part, which we do by means of the analyticity relation

$$\rho = \frac{\Re \mathcal{M}}{\Im \mathcal{M}} = \tan \left[ \frac{\pi}{2} \frac{\partial \log (\Im \mathcal{M} / W^2)}{\partial \log W^2} \right] = \tan \left( \frac{\pi}{2} \Delta_{\mathbf{P}} \right). \quad (2.13)$$

Finally, our amplitude is normalized such, that the differential cross section for  $\gamma p \rightarrow V p$  is

$$\frac{d\sigma(\gamma p \rightarrow V p)}{d\Delta^2} = \frac{1 + \rho^2}{16\pi} \left| \Im m \frac{\mathcal{M}(W, \Delta^2)}{W^2} \right|^2 \exp(-B(W)\Delta^2), \quad (2.14)$$

and thus

$$\sigma_{tot}(\gamma p \rightarrow V p) = \frac{1 + \rho^2}{16\pi B(W)} \left| \Im m \frac{\mathcal{M}(W, \Delta^2)}{W^2} \right|^2. \quad (2.15)$$

## B. $b\bar{b}$ wave function of the $\Upsilon$ meson

We treat the  $\Upsilon, \Upsilon'$  mesons as  $b\bar{b}$   $s$ -wave states, the relevant formalism of light-cone wavefunctions is reviewed in [12]. The vertex for the  $\Upsilon \rightarrow b\bar{b}$  transition is taken as

$$\varepsilon_\mu \bar{u}(p_b) \Gamma^\mu v(p_{\bar{b}}) = [M^2 - M_V^2] \psi_V(z, k^2) \bar{u}(p_b) \left( \gamma^\mu - \frac{p_b^\mu - p_{\bar{b}}^\mu}{M + 2m_b} \right) v(p_{\bar{b}}) \varepsilon_\mu, \quad (2.16)$$

where  $\varepsilon_\mu$  is the polarization vector of the vector meson  $V = \Upsilon, \Upsilon'$ . and  $p_{b,\bar{b}}^\mu$  are the on-shell four-momenta of the  $b, \bar{b}$  quarks,  $p_{b,\bar{b}}^2 = m_b^2$ . The so-defined radial wave-function  $\psi_V(z, k^2)$  can be regarded as a function not of  $z$  and  $k^2$  independently, but rather of the three-momentum  $\vec{p}$  of, say, the quark in the rest frame of the  $b\bar{b}$  system of invariant mass  $M$ ,  $\vec{p} = (\mathbf{k}, (2z - 1)M/2)$ . Then,

$$\psi_V(z, k^2) \rightarrow \psi_V(p^2), \quad \frac{dz d^2 \mathbf{k}}{z(1-z)} \rightarrow \frac{4 d^3 \vec{p}}{M}, \quad p^2 = \frac{M^2 - 4m_b^2}{4}. \quad (2.17)$$

We assume that the Fock-space components of the  $\Upsilon, \Upsilon'$ -states are exhausted by the  $b\bar{b}$  components and impose on the light-cone wave function (LCWF) the orthonormality conditions ( $i, j = \Upsilon, \Upsilon'$ ):

$$\delta_{ij} = N_c \int \frac{d^3 \vec{p}}{(2\pi)^3} 4M \psi_i(p^2) \psi_j(p^2). \quad (2.18)$$

Important constraints on the LCWF are imposed by the decay width  $V \rightarrow e^+ e^-$ :

$$\Gamma(V \rightarrow e^+ e^-) = \frac{4\pi \alpha_{em}^2 c_\Upsilon^2}{3M_V^3} \cdot g_V^2 \cdot K_{NLO}, \quad K_{NLO} = 1 - \frac{16}{3\pi} \alpha_S(m_b^2), \quad (2.19)$$

where ([12, 18])

$$g_V = \frac{8N_c}{3} \int \frac{d^3 \vec{p}}{(2\pi)^3} (M + m_b) \psi_V(p^2). \quad (2.20)$$

For the – fully nonperturbative – LCWF we shall try two different scenarios, following again the suggestions in [12, 18]. Firstly, the Gaussian, harmonic-oscillator-like wave functions:

$$\psi_{1S}(p^2) = C_1 \exp\left(-\frac{p^2 a_1^2}{2}\right), \quad \psi_{2S}(p^2) = C_2(\xi_0 - p^2 a_2^2) \exp\left(-\frac{p^2 a_2^2}{2}\right), \quad (2.21)$$

and secondly, the Coulomb-like wave functions, with a slowly decaying power-like tail:

$$\psi_{1S}(p^2) = \frac{C_1}{\sqrt{M}} \frac{1}{(1 + a_1^2 p^2)^2}, \quad \psi_{2S}(p^2) = \frac{C_2}{\sqrt{M}} \frac{\xi_0 - a_2^2 p^2}{(1 + a_2^2 p^2)^3}. \quad (2.22)$$

The parameters  $a_i^2$  are obtained from fitting the decay widths into  $e^+e^-$ , whereas  $\xi_0$ , and therefore the position of the node of the  $2S$  wave function, is obtained from the orthogonality of the  $2S$  and  $1S$  states. We used the following values for masses and widths:  $M(\Upsilon(1S)) = 9.46$  GeV,  $M(\Upsilon(2S)) = 10.023$  GeV,  $\Gamma(\Upsilon(1S) \rightarrow e^+e^-) = 1.34$  keV,  $\Gamma(\Upsilon(2S) \rightarrow e^+e^-) = 0.61$  keV [19].

### C. Numerical results and comparison with HERA data

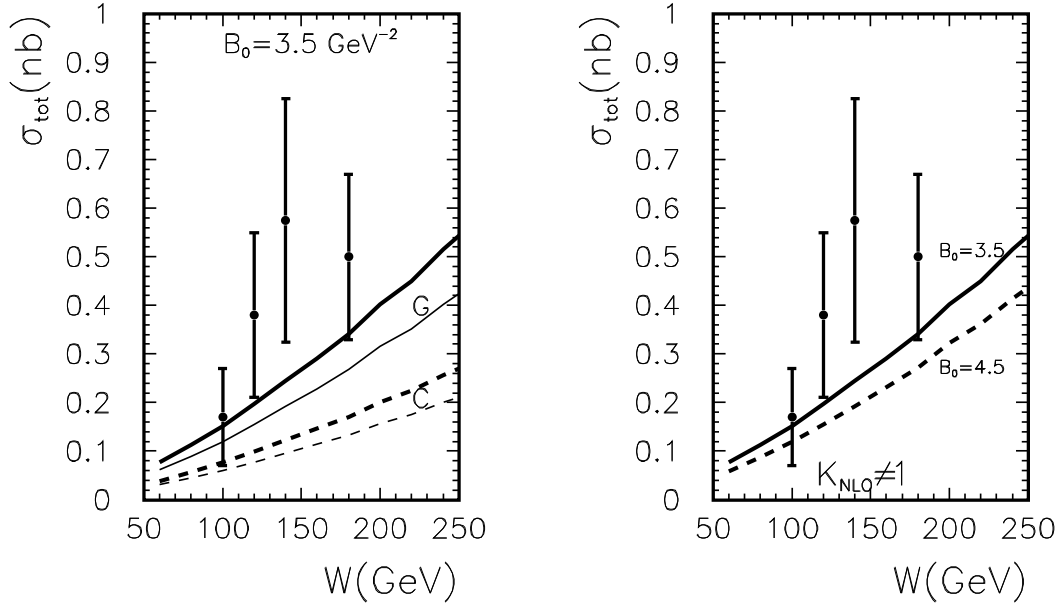


FIG. 2:  $\sigma_{\text{tot}}(\gamma p \rightarrow \Upsilon(1S)p)$  as a function of the  $\gamma p$  cm-energy versus HERA-data. Left: dependence on the treatment of the  $b\bar{b} \rightarrow \Upsilon$  transition; solid curves: Gaussian (G) wave function, dashed curves: Coulomb-like (C) wave function. Thick lines were obtained including the NLO-correction for the  $\Upsilon$  decay width, while for the thin lines  $K_{\text{NLO}} = 1$ . Right: dependence on the slope parameter  $B_0$  (given in  $\text{GeV}^{-2}$ ), for the Gaussian wave function. The experimental data are taken from [9, 10, 11]

In Fig.2 we show the total cross section for the exclusive  $\gamma p \rightarrow \Upsilon p$  process as a function of the  $\gamma p$  cm-energy. In the left panel we show results for two different wave functions discussed

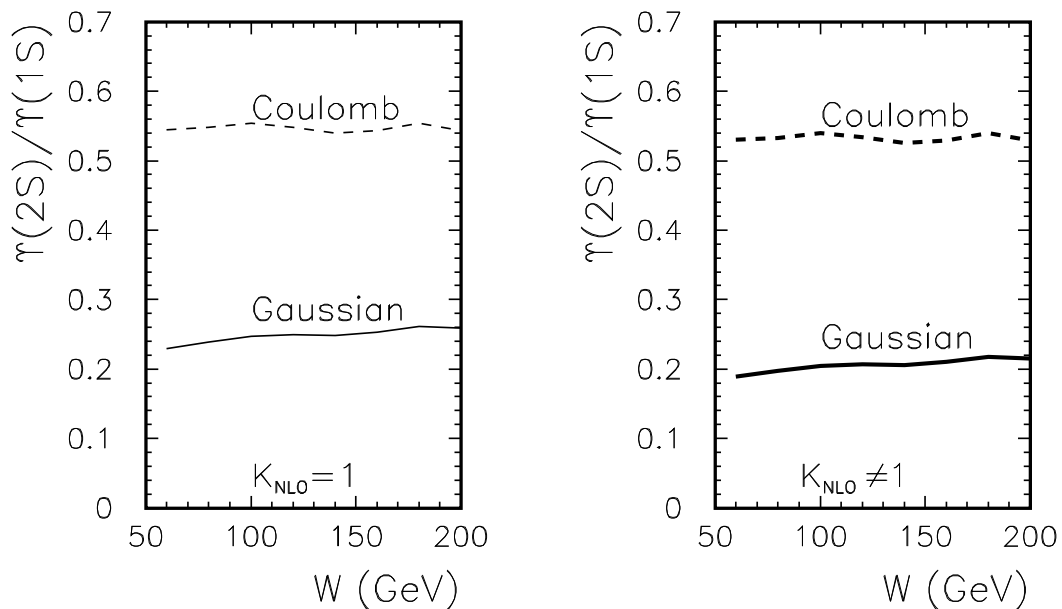


FIG. 3: The  $2S/1S$ -ratio  $\sigma_{tot}(\gamma p \rightarrow \Upsilon(2S)p)/\sigma_{tot}(\gamma p \rightarrow \Upsilon(1S)p)$  as a function of the  $\gamma p$  cm-energy.

in the text: Gaussian (solid lines) and Coulomb-like (dashed lines). Free parameters of the wave function have been adjusted to reproduce the leptonic decay width in two ways: (a) using leading order formula (thin lines) and (b) including QCD corrections (thick lines). Including the  $K_{NLO}$ -factor in the width enhances the momentum-space integral over the wave function (the WF at the spatial origin), and hence enhances the prediction for the photoproduction cross section. Notice that strictly speaking inclusion of the  $\alpha_S$ -correction is not really warranted given that we do not have the corresponding radiative corrections to the production amplitude. Fortunately, due to the large scale  $m_b^2$ , the ambiguity in the two ways of adjusting the wave function parameters leads to only a marginal difference in the total cross section over most of the relevant energy range. To be fair, it should be mentioned, that the situation with the next-to-leading order corrections to diffractive vector mesons is not a very comfortable one, see for example the instabilities reported in [20]. But then, the systematic extension of  $k_\perp$ -factorisation is yet lacking, so that at present we must be content with estimates of the theoretical uncertainties obtained by changing the principal parameters in the calculation.

As can be seen from the figure, different functional forms of the LCWF can lead to a quite substantial differences in the predicted cross section. Finally, the absence of experimental data for  $t$ -distributions leaves the slope parameter  $B_0$  only badly constrained. The full, energy dependent slope can be decomposed into three contributions: one from the transition  $\gamma \rightarrow V$ , a second one from the dynamics of the gluon ladder exchanged – which induces the main part of its energy dependence, and a third one from the elastic  $p \rightarrow p$  vertex. In comparison to  $J/\psi$ -production, we may expect, that the slope in our case receives a smaller contribution from the  $\gamma \rightarrow V$  transition, due to the smaller transverse sizes involved [21]. It may therefore be expected that  $B_0$  should be somewhat smaller than in  $J/\Psi$  photoproduction, where it is  $\sim 4.6 \text{ GeV}^{-2}$  [16].

We show the sensitivity to the slope parameter  $B_0$  in the right panel of Fig.2.

We observe, that in general our predictions are systematically somewhat below the experimental data. In principle, the agreement could be improved by choosing an abnormally small value for  $B_0$ , we shall however refrain from such an option. In our view the description of data, given the large error bars, is quite acceptable. The energy dependence of our result corresponds to an effective  $\Delta_{\mathbf{p}} \sim 0.39$ . For our predictions for Tevatron we shall use the Gaussian LCWF option, with the NLO correction to the width included.

In Fig.3 we show the ratio of the cross section for the first radial excitation  $\Upsilon(2S)$  to the cross section for the ground state  $\Upsilon(1S)$ . The principal reason behind the suppression of the  $2S$  state is the well-known node effect (see [22] and references therein) – a cancellation of strength in the  $2S$  case due to the change of sign of the radial wave function. It is perhaps not surprising, that the numerical value of the  $2S/1S$ -ratio is strongly sensitive to the shape of the radial light-cone wave function.

Here we assumed an equality of the slopes for  $\Upsilon(1S)$  and  $\Upsilon(2S)$  production. This appears to be justified, given the large spread of predictions from different wave functions. We finally note, that the ratio depends very little on the choice of the  $K_{NLO}$  factor (compare left and right panel).

### III. EXCLUSIVE PHOTOPRODUCTION IN $p\bar{p}$ COLLISIONS

#### A. The absorbed $2 \rightarrow 3$ amplitude

The necessary formalism for the calculation of amplitudes and cross-sections was outlined in sufficient detail in Ref. [7]. Here we give only a brief summary. The basic mechanisms are shown in Fig.4. The major difference from HERA, where the photon was emitted

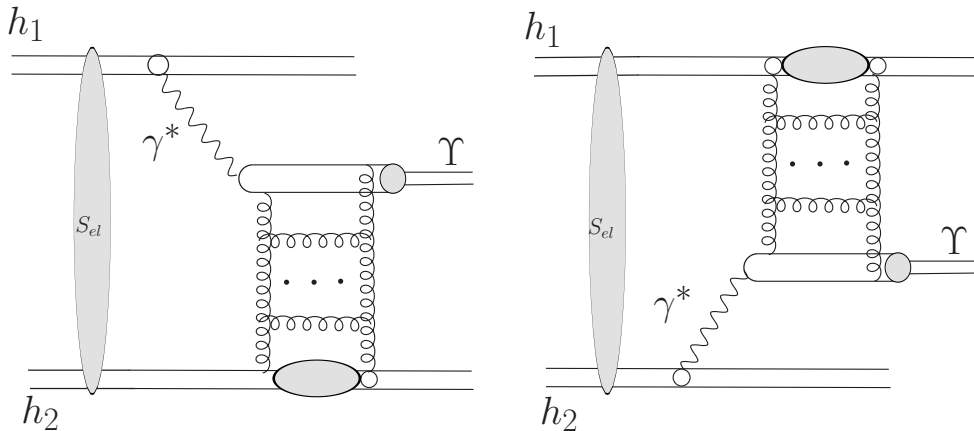


FIG. 4: A sketch of the two mechanisms considered in the present paper: photon-pomeron (left) and pomeron-photon (right), including absorptive corrections.

by a lepton which does not participate in the strong interactions, now, both initial state hadrons can be the source of the photon. Therefore, it is now necessary to take account of the interference between two amplitudes. The photon exchange parts of the amplitude, involve only very small, predominantly transverse momentum transfers. In fact, here we concentrate on the kinematic domain, where the outgoing protons lose only tiny fractions



$z_1, z_2 \ll 1$  of their longitudinal momenta, in practice  $z \lesssim 0.1$  means  $y \lesssim 3$ . In terms of the transverse momenta of outgoing hadrons,  $\mathbf{p}_{1,2}$ , the relevant four-momentum transfers are  $t_i = -(\mathbf{p}_i^2 + z_i^2 m_p^2)/(1 - z_i)$ ,  $i = 1, 2$ , and  $s_1 \approx (1 - z_2)s$  and  $s_2 \approx (1 - z_1)s$  are the familiar Mandelstam variables for the appropriate subsystems. Photon virtualities  $Q_i^2$  are small (what counts here is that  $Q_i^2 \ll M_Y^2$ ), so that the contribution from longitudinal photons can be safely neglected. Also, as mentioned above, we assume the  $s$ -channel-helicity conservation in the  $\gamma^* \rightarrow \Upsilon$  transition. In summary we present the  $2 \rightarrow 3$  Born-amplitude (without absorptive corrections) in the form of a two-dimensional vector (corresponding to the two transverse (linear) polarizations of the final state vector meson):

$$\mathbf{M}^{(0)}(\mathbf{p}_1, \mathbf{p}_2) = e_1 \frac{2}{z_1} \frac{\mathbf{p}_1}{t_1} \mathcal{F}_{\lambda'_1 \lambda_1}(\mathbf{p}_1, t_1) \mathcal{M}_{\gamma^* h_2 \rightarrow V h_2}(s_2, t_2, Q_1^2) + (1 \leftrightarrow 2) \quad (3.1)$$

Inclusion of absorptive corrections (the 'elastic rescattering') leads in momentum space to the full, absorbed amplitude

$$\mathbf{M}(\mathbf{p}_1, \mathbf{p}_2) = \int \frac{d^2 \mathbf{k}}{(2\pi)^2} S_{el}(\mathbf{k}) \mathbf{M}^{(0)}(\mathbf{p}_1 - \mathbf{k}, \mathbf{p}_2 + \mathbf{k}) = \mathbf{M}^{(0)}(\mathbf{p}_1, \mathbf{p}_2) - \delta \mathbf{M}(\mathbf{p}_1, \mathbf{p}_2). \quad (3.2)$$

With

$$S_{el}(\mathbf{k}) = (2\pi)^2 \delta^{(2)}(\mathbf{k}) - \frac{1}{2} T(\mathbf{k}), \quad T(\mathbf{k}) = \sigma_{tot}^{p\bar{p}}(s) \exp\left(-\frac{1}{2} B_{el} \mathbf{k}^2\right), \quad (3.3)$$

where  $\sigma_{tot}^{p\bar{p}}(s) = 76 \text{ mb}$ ,  $B_{el} = 17 \text{ GeV}^{-2}$  [23], the absorptive correction  $\delta \mathbf{M}$  reads

$$\delta \mathbf{M}(\mathbf{p}_1, \mathbf{p}_2) = \int \frac{d^2 \mathbf{k}}{2(2\pi)^2} T(\mathbf{k}) \mathbf{M}^{(0)}(\mathbf{p}_1 - \mathbf{k}, \mathbf{p}_2 + \mathbf{k}). \quad (3.4)$$

The differential cross section is given in terms of  $\mathbf{M}$  as

$$d\sigma = \frac{1}{512\pi^4 s^2} |\mathbf{M}|^2 dy dt_1 dt_2 d\phi, \quad (3.5)$$

where  $y$  is the rapidity of the vector meson, and  $\phi$  is the angle between  $\mathbf{p}_1$  and  $\mathbf{p}_2$ .

## B. Results for Tevatron

We now come to the results of differential cross sections for  $\Upsilon$  production. In Fig.5 we show the distribution in rapidity of  $\Upsilon(1S)$  (left panel) and  $\Upsilon(2S)$  (right panel). The ratio between  $2S$  and  $1S$  follows closely the photoproduction ratio discussed in Sec. II C. The parameters chosen for this calculation correspond to the Gaussian wave function, with  $K_{NLO}$  included in the adjustment to the decay width. Also the unintegrated gluon distribution is the same as the one used in section II C. The results obtained with bare amplitudes are shown by the thin (red) lines, and the results with absorption effects included are shown by thick (black) lines. Here the absorption effects are truly a correction and cause only about 20-30% decrease of the cross section. This is in sharp contrast to the situation for the fusion of two QCD ladders (relevant for the production of scalar charmonia or Higgs boson). The rapidity distribution is only slightly distorted by absorptive corrections. Notice that larger

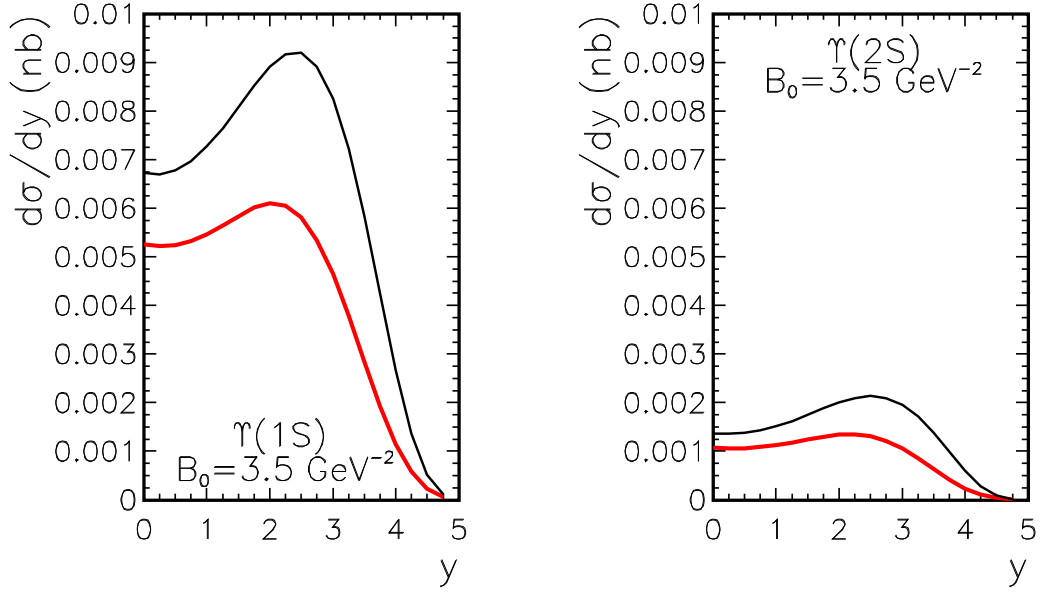


FIG. 5: Differential cross section  $d\sigma/dy$  for  $\Upsilon(1S)$  (left panel) and  $\Upsilon(2S)$  (right panel) for the Tevatron energy  $W = 1960$  GeV. The thin solid line is for the calculation with bare amplitude, the thick line for the calculation with absorption effects included.

rapidities mean also larger photon virtualities and therefore somewhat smaller transverse distances in the  $p\bar{p}$  collision are relevant.

Finally, in the following figures we show distributions of  $\Upsilon$ 's in transverse momentum. We show results for different values of rapidity:  $y = 0$  (solid),  $y = 2$  (dashed) and  $y = 4$  (dotted). In Fig.6 we show the distributions for  $\Upsilon(1S)$  and in Fig.7 for  $\Upsilon(2S)$ . Both, results with bare amplitudes (left panels), and with absorption (right panels) are shown. The inspection of the figures shows that absorption effects are larger for large values of the  $\Upsilon$  transverse momenta – they can lower the cross section by almost an order of magnitude at the largest transverse momenta. There is again a different effect of absorption for different rapidities.

Notice, that our predictions, which use the low- $z$  approximation of the photon flux are most accurate at  $y \lesssim 3$ . This is quite appropriate for Tevatron, where it seems that a measurement is possible only at rather low rapidities. We do not show here observables related to outgoing proton or/and antiproton as they cannot be studied experimentally at the Tevatron. There will be, however, such a possibility at the LHC.

There are important issues regarding the extrapolation to LHC energies. Firstly the energy of the  $\gamma p \rightarrow \Upsilon p$  process can vastly exceed the HERA range, and secondly the much increased rapidity range may increase the importance of high-mass diffraction for the absorptive corrections. Still, to give the reader a rough idea of the expected cross section, we show in Fig. 8 selected spectra at the LHC energy of  $W = 14$  TeV. Here, in the absorptive corrections, we used a Pomeron intercept of  $\Delta_{\mathbf{P}} = 0.08$ . It is interesting to point out that the rise towards the maximum in the rapidity distribution reflects the energy dependence of the  $\gamma p \rightarrow \Upsilon p$  subprocess. Absorptive corrections in that subprocess, which we neglected so far can possibly alter the shape of the rapidity distribution. Since there are many other

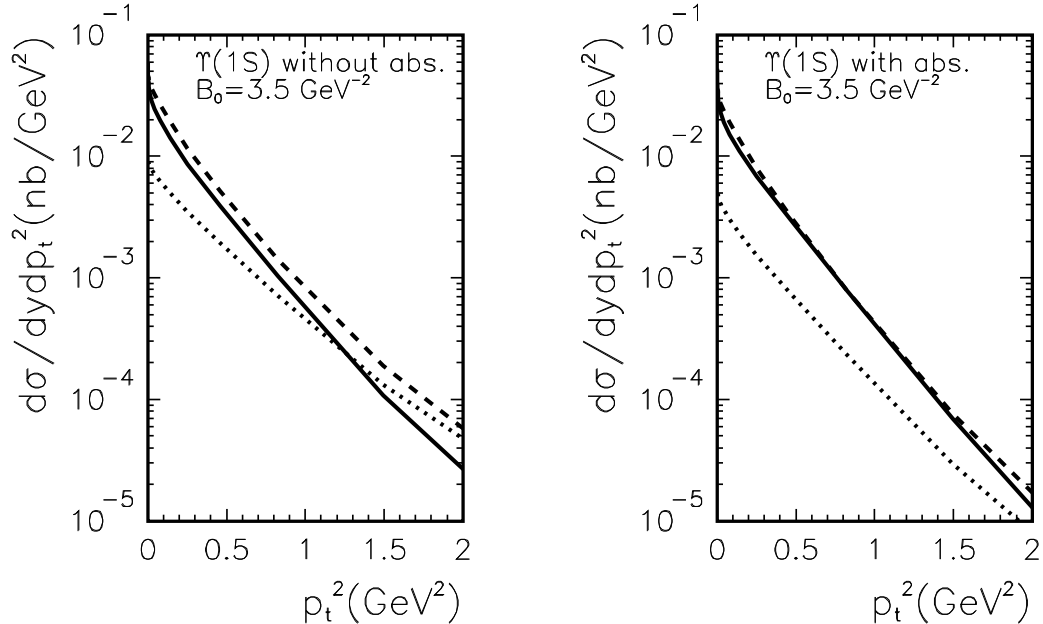


FIG. 6: Invariant cross section  $d\sigma/dydp_t^2$  for  $\Upsilon(1S)$  for  $W = 1960$  GeV. The solid line:  $y = 0$ , dashed line:  $y = 2$ , dotted line:  $y = 4$ . Left panel: without absorptive corrections; Right panel: with absorptive corrections.

interesting aspects at larger energies we leave a more detailed analysis for LHC for a separate publication.

A brief comment on previous works is in order. In [4, 6, 8] absorptive corrections were not included. The equivalent photon approximation is used in [4, 8], which allows only to obtain rapidity spectra. The form of the transverse momentum distribution suggested in [4] is not borne out by our calculation. Cross sections  $d\sigma/dy$  obtained in [4, 6, 8] lie in the same ballpark as the results presented here. However the shape of the rapidity distribution in [8] is different from ours.

#### IV. CONCLUSIONS

We have calculated the forward amplitude for  $\gamma p \rightarrow \Upsilon p$  reaction within the formalism of  $k_\perp$ -factorization. In this approach the energy dependence of the process is encoded in the  $x$ -dependence of unintegrated gluon distributions. The latter object is constrained by data on inclusive deep inelastic scattering. The  $t$ -dependence for the  $\gamma p \rightarrow \Upsilon p$  process involves a free parameter and is in effect parametrized. Regarding the  $\gamma \rightarrow \Upsilon$  transition, we used different Ansätze for the  $b\bar{b}$  wave functions. The results for  $\Upsilon(1S)$  production depend only slightly on the model of the wave function, while the  $2S/1S$  ratio shows a substantial sensitivity. We compared our results for the total cross section with a recent data from HERA. Our results are systematically somewhat lower than data, although the overall discrepancy is not worrisome, given the large uncertainties due to the rather poor experimental resolution in the meson mass. The amplitudes for the  $\gamma p \rightarrow \Upsilon p$  process are

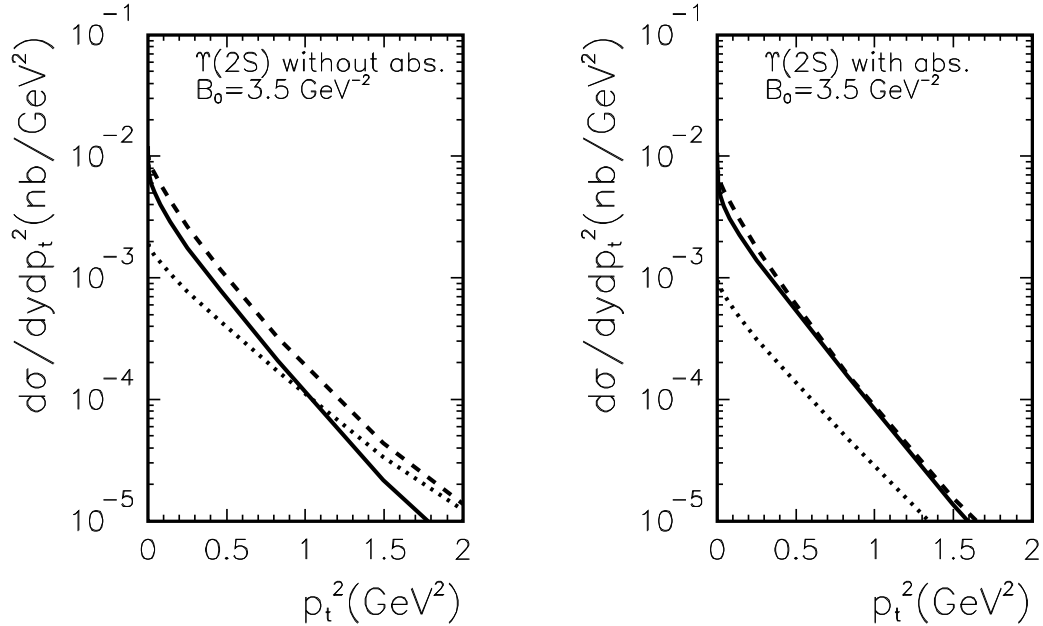


FIG. 7: Invariant cross section  $d\sigma/dydp_t^2$  as a function of  $p_t^2$  for  $\Upsilon(2S)$  for  $W = 1960$  GeV. The solid line:  $y = 0$ , dashed line:  $y = 2$ , dotted line:  $y = 4$ . Left panel: without absorptive corrections; Right panel: with absorptive corrections.

used next to calculate the amplitude for the  $p\bar{p} \rightarrow p\bar{p}\Upsilon$  reaction assuming the photon-Pomeron (Pomeron-photon) underlying dynamics. In the present approach the Pomeron is then described within QCD in terms of unintegrated gluon distributions. We have calculated several differential distributions including soft absorption effects not included so far in the literature. Our predictions are relevant for current experiments at the Tevatron, predictions were made – with qualifications – for possible future experiments at the LHC.

## V. ACKNOWLEDGEMENTS

This work was partially supported by the Polish Ministry of Science and Higher Education (MNiSW) under contract 1916/B/H03/2008/34.

- 
- [1] M. Krämer, Prog. Part. Nucl. Phys. **47** (2001) 141; J.P. Lansberg, Int. J. Mod. Phys. **A21** (2006) 3857.
  - [2] A. Schäfer, L. Mankiewicz and O. Nachtmann, Phys. Lett. B **272**, 419 (1991).
  - [3] V. A. Khoze, A. D. Martin and M. G. Ryskin, Eur. Phys. J. C **24**, 459 (2002).
  - [4] S. R. Klein and J. Nystrand, Phys. Rev. Lett. **92**, 142003 (2004).
  - [5] V. P. Goncalves and M. V. T. Machado, Eur. Phys. J. C **40**, 519 (2005).
  - [6] A. Bzdak, L. Motyka, L. Szymanowski and J. R. Cudell, Phys. Rev. D **75**, 094023 (2007).
  - [7] W. Schäfer and A. Szczurek, Phys. Rev. D **76**, 094014 (2007).

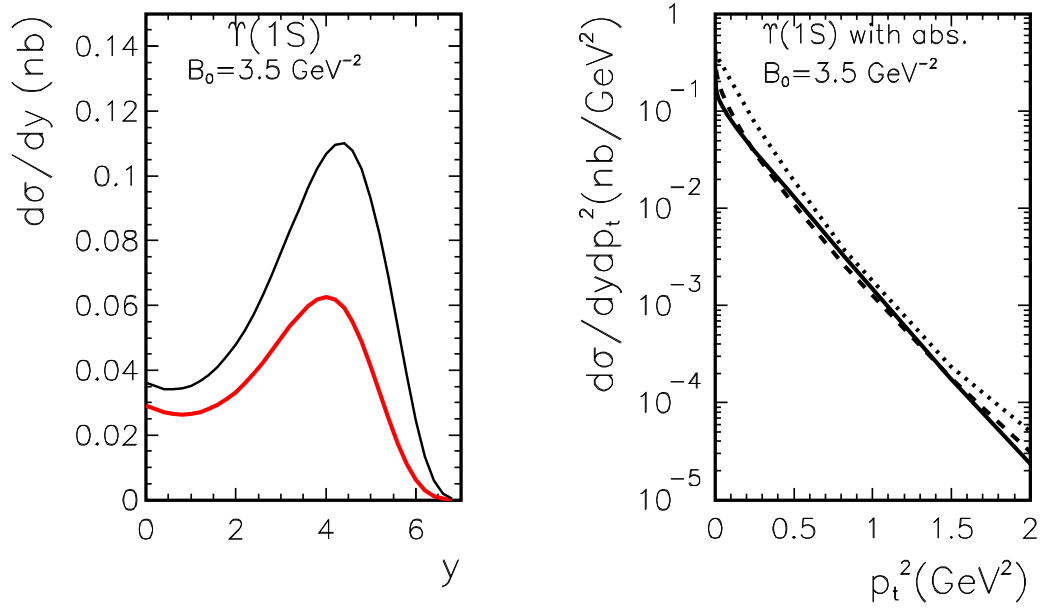


FIG. 8: Left panel: differential cross section  $d\sigma/dy$  for  $\Upsilon(1S)$  for the LHC energy  $W = 14$  TeV. The thin solid line: without absorptive corrections; thick line: with absorptive corrections. Right panel: invariant cross section  $d\sigma/dy dp_t^2$  for  $\Upsilon(1S)$  as a function of  $p_t^2$  for  $W = 14$  TeV. The solid line:  $y = 0$ , dashed line:  $y = 2$ , dotted line:  $y = 4$ . Absorptive corrections are included.

- [8] V. P. Goncalves and M. V. T. Machado, Phys. Rev. D **77**, 014037 (2008).
- [9] J. Breitweg *et al.* [ZEUS Collaboration], Phys. Lett. B **437**, 432 (1998).
- [10] C. Adloff *et al.* [H1 Collaboration], Phys. Lett. B **483**, 23 (2000).
- [11] I. Rubinskiy for the H1 and ZEUS Collaborations, “Exclusive Processes in ep collision at HERA”, a talk at the International Europhysics Conference On High Energy Physics (EPS-HEP2007), Manchester, England, 19-25 July 2007.
- [12] I. P. Ivanov, N. N. Nikolaev and A. A. Savin, Phys. Part. Nucl. **37**, 1 (2006).
- [13] I. P. Ivanov and N. N. Nikolaev, Phys. Rev. D **65**, 054004 (2002).
- [14] J. R. Andersen *et al.* [Small x Collaboration], Eur. Phys. J. C **48** (2006) 53; M. Łuszczak and A. Szczurek, Phys. Rev. D **73** (2006) 054028; A. Szczurek, Acta Phys. Polon. B **34** (2003) 3191.
- [15] J. Pinfold, a talk at Photon 2007: International Conference on the Structure and Interactions of the Photon and the 17th International Workshop on Photon-Photon Collisions and International Workshop on High Energy Photon Linear Colliders, Paris, France, 9-13 Jul 2007.
- [16] A. Aktas *et al.* [H1 Collaboration], Eur. Phys. J. C **46**, 585 (2006).
- [17] A. G. Shuvaev, K. J. Golec-Biernat, A. D. Martin and M. G. Ryskin, Phys. Rev. D **60**, 014015 (1999).
- [18] I. P. Ivanov, “Diffractive production of vector mesons in deep inelastic scattering within  $k(t)$ -factorization approach,” arXiv:hep-ph/0303053.
- [19] W. M. Yao *et al.* [Particle Data Group], J. Phys. G **33**, 1 (2006).
- [20] D. Y. Ivanov, A. Schäfer, L. Szymanowski and G. Krasnikov, Eur. Phys. J. C **34**, 297 (2004).

- [21] J. Nemchik, N. N. Nikolaev, E. Predazzi, B. G. Zakharov and V. R. Zoller, J. Exp. Theor. Phys. **86**, 1054 (1998) [Zh. Eksp. Teor. Fiz. **113**, 1930 (1998)].
- [22] J. Nemchik, N. N. Nikolaev, E. Predazzi and B. G. Zakharov, Z. Phys. C **75**, 71 (1997)
- [23] F. Abe *et al.* [CDF Collaboration], Phys. Rev. D **50**, 5518 (1994).